Thermal Properties of Mixed Alkali Bis(trifluoromethylsulfonyl)amides

Hagiwara, Rika; Tamaki, Kenichiro; Kubota, Keigo; Goto, Takuya; Nohira, Toshiyuki

Thermal properties of mixed alkali bis(trifluoromethylsulfonyl)amides

Rika Hagiwara, Kenichiro Tamaki, Keigo Kubota, Takuya Goto, Toshiyuki Nohira

Graduate School of Energy Science, Kyoto University

Sakyo-ku, Kyoto 606-8501, Japan

Phase diagrams of binary mixtures of alkali bis(trifluoromethylsulfonyl)amides have been constructed and their eutectic compositions and temperatures have been determined. It has been revealed that the molten salt electrolytes having the melting points in the intermediate temperature range (373 to 473) K are easily formed by simple mixing of two kinds of single alkali bis(trifluoromethylsulfonyl)amides salts. The 1:1 or 3:1 double salt is occasionally formed for some binary systems.

Introduction

Molten salts have excellent characteristics as electrolytes such as negligibly small volatility, non-flammability, high electrochemical stability and high ionic conductivity[1-2]. Molten salts are roughly classified into two groups: high temperature molten salts (T > 673 K) and room (or ambient) temperature molten salts (T < 373 K). There is a trade-off between the features as electrolytes for the high temperature and room temperature molten salts. High temperature molten salts are generally superior in physicochemical properties such as high conductivities, wide electrochemical windows and wide liquid temperature range. On the other hand, the room temperature molten salts, also called ionic liquids, have the advantages of an easy handling and wide range of application field[3-6]. Salts consisting of alkali metal cations and bis(trifluoromethylsulfonyl)amide (Tf_2N) anion, MTf_2N (M = Li, Na, K, Rb, Cs) are solids at room temperature, but have, or are expected to have, melting points at relatively low temperatures[7-8] . The Tf_2N anion is well known as one of the major anions constituting room temperature molten salts because of its high chemical and electrochemical stability[9].

It would be possible to obtain molten salts having melting points of lower than those of the single MTf_2N salts from their mixture. These molten salt mixtures are expected to have melting points from (373 to 473) K and be used at intermediate temperatures (373 to 673) K, giving averaged characteristics of high temperature and room temperature molten salts. It is also expected that the alkali metal Tf_2N salts are promising as intermediate temperature molten salt electrolytes for electrochemical systems including a process of alkali metal depositions owing to the high electrochemical stability of Tf_2N anion. For example, lithium metal is expected to deposit at the cathode limit of mixed MTf_2N molten salts containing $LiTf_2N$ and these molten salts are able to be used as electrolytes for lithium ion batteries operating at intermediate temperatures.

Many researchers have reported organic electrolytes for lithium ion batteries in which $LiTf_2N$ is dissolved as supporting electrolytes[10-12], however, the properties reported for MTf_2N salts themselves are limited except for some crystal structures[13]. No reports are available on the physicochemical properties of the molten MTf_2N salts and their mixtures.

In this study, the thermal properties of the mixtures of the two MTf_2N single salts (M = Li, Na, K, Rb, Cs) were systematically investigated to construct phase

diagrams and determine the composition giving the melting points in the intermediate temperature range.

Experimental Section

Bis(trifluoromethylsulfonyl)imide, HTf_2N (Morita Chemical Industries, purity > 99 %), Na_2CO_3 (Wako Pure Chemical Industries, purity > 99.5 %), K_2CO_3 (Wako Pure Chemical Industries, purity 99.9 %), Rb_2CO_3 (Wako Pure Chemical Industries, purity 99.9 %) and Cs_2CO_3 (Aldrich, purity 99.9 %) were used for the syntheses of MTf_2N salts. $LiTf_2N$ (Morita Chemical Industries, purity > 99.0 %) was used as received. Melting points and thermal decomposition temperatures of single MTf_2N salts were measured by means of differential scanning calorimetry (DSC) and thermogravimetry (TG), respectively. Temperature was increased with a scan rate of 10 K min^{-1}. The phase diagrams of the binary MTf_2N salt mixtures were constructed by plotting the temperatures of endothermic peaks found on the DSC curves obtained in the heating process against the compositions of the salts. The transition temperatures were determined in heating process in order to avoid uncertainty by supercooling. The liquidus and solidus curves were drawn by eye through experimental plots. The

measurements were performed for the rate 5 %. Aluminum pans were used for the sample holders. Prior to the measurements, the sample was melted at 573 K in order to prepare homogenous samples. The measurement was started after cooling the pre-treated samples down to room temperature. In this study, accuracy of melting points is ±5 K.

Results and discussion

Melting and thermal decomposition temperatures of single MTf_2N salts

The melting and thermal decomposition temperatures of MTf_2N single salts in this study are summarized in Table 1. Figure 1 shows the plots of the melting points of the single salts against the reciprocal radii of the cations. Coordination numbers of the cations ($LiTf_2N$: 6, $NaTf_2N$: 6, KTf_2N: 8 $RbTf_2N$: 8, $CsTf_2N$: 10) from the previous study on the crystal structure of the MTf_2N salts[13] are used to estimate the ionic radii of the cations. The melting point of the salt containing a smaller cation is generally higher, but it is found from the figure that the melting point of $LiTf_2N$ does not follow the trend, irregularly lower than that of $NaTf_2N$. This would be caused by the difference of the

lattice energies of the salts with different structures containing a large organic anion in which the electrostatic interactions are more complicated than that in simple inorganic salts. The single MTf_2N salts are thermally stable to 700 K except for $LiTF_2N$ of which the decomposition temperature is 657 K. Thermal stability becomes higher with the increase of the size of the cation.

Phase diagrams of the binary MTf_2N salt mixtures

Figure 2 shows a phase diagram of $LiTf_2N$ + $NaTf_2N$ binary system that exhibits a simple binary eutectic system. Figure 3 shows a phase diagram of $NaTf_2N$ + $RbTf_2N$ binary system. The phase diagram is also a simple eutectic type. No binary compounds and structural phase transition are observed. These two systems are a simple eutectic type in the binary MTf_2N systems examined here.

Figure 4 shows a phase diagram of KTf_2N + $CsTf_2N$. There are two endothermic peaks on the DSC curves at different temperatures at $X_{KTf2N} \geq 0.25$. Although only one peak is observed at $X_{KTf2N} \leq 0.20$, the system is considered to be a simple eutectic type. It is considered that the eutectic composition is very close to the $CsTf_2N$ side, and that the eutectic temperature is almost equal to the melting point of

$CsTf_2N$.

Figure 5 illustrates a phase diagram of $LiTf_2N$ + $RbTf_2N$ system. The endothermic peak found at the lowest temperature, 421 K, shifts by 5 K to a higher temperature, 426 K, at $X_{LiTf2N} > 0.50$. At this composition, only one endothermic peak is observed at 432 K. This suggests the existence of a double salt, $LiRb(Tf_2N)_2$. As a result, this binary system has two eutectic points. A similar phase diagram is found for $LiTF_2N$-$CsTF_2N$ binary system as shown in Figure 6. The endothermic peak at 385 K appears only at the compositions where the molar ratios of $LiTf_2N$ are 0.05 to 0.50 and this peak disappears for the higher $LiTf_2N$ compositions. This suggests the existence of a double salt, $LiCs(Tf_2N)_2$. As a result, this binary system has two eutectic points in common with the $LiTf_2N$ + $RbTf_2N$. Formation of 1:1 double salts is suggested for these two systems.

A phase diagram of $LiTf_2N$ + KTf_2N binary system is shown in Figure 7. Two endothermic peaks are observed when the molar ratio of $LiTf_2N$ exceeds 0.75. These observations suggest the existence of the 3:1 double salt, $Li_3K(TF_2N)_4$. A peritectic point should exist at $X_{LiTf2N} \simeq 0.7$ with the temperature of 435 K. The eutectic point is found at $X_{LiTf2N} = 0.43$ with the temperature of 423 K. A similar phase diagram is obtained for $NaTf_2N$ + KTf_2N binary system and shown in Figure 8. There is a

peritectic point at X_{NaTf2N} = 0.45 at a temperatures of 462 K. Three endothermic peaks also appear at $X_{NaTf2N} \geq 0.45$. Similarly, it suggests the formation of a 3:1 double salt, $Na_3K(Tf_2N)_4$. Figure 9 illustrates a phase diagram of $NaTf_2N$ + $CsTf_2N$. The endothermic peak at 383 K disappears at $X_{NaTf2N} \geq 0.75$. It suggests the formation of a 3:1 double salt, $Na_3Cs(Tf_2N)_4$. A peritectic point is found at X_{NaTf2N} = 0.22 with the temperature of 411 K.

Table 2 summarizes the eutectic compositions and temperatures of binary MTf_2N salt mixtures. Table 3 summarizes the intermediate compounds of binary MTf_2N salt mixtures.

In the case of KTf_2N + $RbTf_2N$ binary system, as shown in Fig. 10, only one endothermic peak is observed for entire compositions in the DSC curves. It is, thus, impossible to obtain the compositions having lower melting point than neat $RbTf_2N$ by the mixing of KTf_2N and $RbTf_2N$. The $RbTf_2N$ + $CsTf_2N$ system, as shown in Figure 11, is similar to the KTf_2N-$RbTf_2N$ system. In this binary system, again there is only one endothermic peak at different temperatures for all mole fractures. It is concluded that these two systems form solid solutions for all mole fractures. In these systems, it is considered that there are two-phase regions where liquid and solid solution exist between liquidus and solidus. However the regions could not be detected in this

measurement.

It is found that the melting points are not lowered in the case of KTf_2N + $RbTf_2N$, KTF_2N + $CsTF_2N$ and $RbTf_2N$ + $CsTf_2N$ binary systems in which the two of the three heaviest alkali metal salts are mixed. When the cation sizes are close (K: 1.51 Å, Rb: 1.61 Å, Cs: 1.81 Å), the binary salt system might behave as a pseudo single phase although the melting temperature shifts with the composition.

Conclusions

Thermal properties of the binary MTf_2N (M = Li, Na, K, Rb, Cs) salt mixtures were investigated. Ten binary phase diagrams have been constructed. In the cases of the seven binary salt mixtures, the melting points are lowered to intermediate temperatures (373 to 473) K by the mixing of two single MTf_2N salts. Thus the mixing of alkali metal Tf_2N salt is an effective way to lower the melting temperature of alkali metal Tf_2N salts except for a few combinations.

Literature Cited

(1) Ito, Y.; Nohira, T. Non-conventional Electrolytes for Electrochemical Applications. *Electrochim. Acta* **2000**, *45*, 2611-2622.

(2) Galasiu, I.; Galasiu, R.; Thonstad, J. *Electrochemistry of Molten Salts*, In *Nonaqueous Electrochemistry, Chapt. 9,* Aurbach, D. ed.; Marcel Dekker, New York, 1999; pp 461-591.

(3) *Ionic Liquids in Synthesis*. Holbrey, J.D.; Rogers, R. D. eds.; VCH-Wiley, Weinheim, 2002.

(4) *Green Industrial Applications of Ionic Liquids*. Rogers, R.D.; Seddon, K.R.; Volkov, S. eds.; Kluwer Academic Publishers, 2003.

(5) *Electrochemical Aspects of Ionic Liquids*. Ohno, H.ed.; John Wiley & Sons, Inc., 2005.

(6) Hagiwara, R.; Lee, J, S. Ionic Liquids for Electrochemical Devices. *Electrochemistry* **2007**, *75*, 23-34.

(7) Lascaud, S.; Perrier, M.; Vallée, A.; Besner, S.; Prud'homme', J.; Armand, J. Phase Diagrams and Conductivity Behavior of Poly(Ethylene Oxide)-Molten Salt Rubbery Electrolytes. *Macromolecules* **1994,** *27*, 7469-7477.

(8) Foropoulos, J.; DesMarteau, D. D. Synthesis, Properties, and Reactions Bis((trifluoromethyl)sulfonyl)Imide, $(CF_3SO_2)_2NH$. *Inorg. Chem.* **1984**, *23*, 3720-3723.

(9) Bonhôte, P.;Dias, A-P.; Armand, M.; Papageorgiou, N.; Kalyanasundaram, K.; Grätzel, M. Hydrophobic, Highly Conductive Ambient-Temperature Molten Salts. *Inorg. Chem.* **1996**, *35,* 1168-1178.

(10) Matsumoto, H.; Yanagida, M.;Tanimoto, K.; Kojima, T.; Tamiya, Y.; Miyazaki, Y. Improvement of Ionic Conductivity of Room Temperature Molten Salt Based on Quaternary Ammonium Cation and Imide Anion. *Proceedings - Electrochemical Society* **2000**, *99-41*, 186-192.

(11) Koura, N.; Etoh, K.; Idemoto, Y.; Matsumoto, F. Electrochemical Behavior of Graphite-Lithium Intercalation Electrode in $AlCl_3$-EMIC-LiCl-$SOCl_2$ Room-Temperature Molten Salt. *Chemistry Letters* **2001**, 1320-1321.

(12) Sakaebe, H.; Matsumoto, H. *N*-Methyl-*N*-Propylpiperidinium Bis(Trifluoromethanesulfonyl)Imide (PP13-TFSI) - Novel Electrolyte Base for Li Battery. *Electrochemistry Communications* **2003**, *5*, 594-598.

(13) Xue, L.; Padgett, C. W.; DesMarteau, D. D.; Pennington, W.T. Synthesis and Structures of Alkali Metal Salts of Bis[(Trifluoromethyl)sulfonyl]Imide. *Solid State Sciences* **2002,** *4*, 1535-1545.

Table 1. Melting temperature T, and decomposition temperatures T_d, of MTf_2N single salts.

	$LiTf_2N$	$NaTf_2N$	KTf_2N	$RbTf_2N$	$CsTf_2N$
T/K (this study)	506	530	472	450	395
T/K (previous study)	507 [7]	-	478 [7]	-	388 [8]
T_d/K	657	714	733	740	745

Table 2. Eutectic compositions, x_{eu} and temperatures, T_{eu} of the binary MTf_2N salt mixtures.

System	x_{eu}	T_{eu}/K
$LiTf_2N + NaTf_2N$	$x_{LiTf2N} = 0.67$	453
$LiTf_2N + KTf_2N$	$x_{LiTf2N} = 0.43$	423
$KTf_2N + CsTf_2N$	-	395
$LiTf_2N + RbTf_2N$	$x_{LiTf2N} = 0.25$	421
	$= 0.60$	426
$LiTf_2N + CsTf_2N$	$x_{LiTf2N} = 0.07$	385
	$= 0.60$	432
$NaTf_2N + KTf_2N$	$x_{NaTf2N} = 0.25$	456
$NaTf_2N + RbTf_2N$	$x_{NaTf2N} = 0.25$	431
$NaTf_2N + CsTf_2N$	$x_{NaTf2N} = 0.07$	383

Table 3. Intermediate compounds of the binary MTf_2N salt mixtures.

System	Compound
$LiTf_2N + RbTf_2N$	$LiRb(Tf_2N)_2$
$LiTf_2N + CsTf_2N$	$LiCs(Tf_2N)_2$
$LiTf_2N + KTf_2N$	$Li_3K(Tf_2N)_4$
$NaTf_2N + KTf_2N$	$Na_3K(Tf_2N)_4$
$NaTf_2N + CsTf_2N$	$Na_3Cs(Tf_2N)_4$

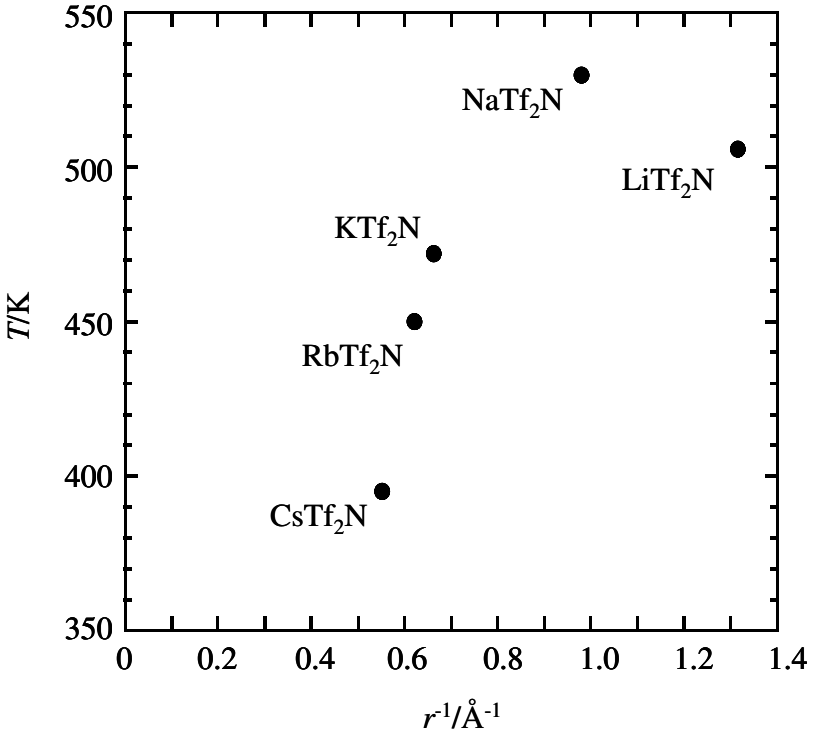

Figure 1. Plots of the melting temperature, T against the reciprocal radius of the cations of the salts, r.

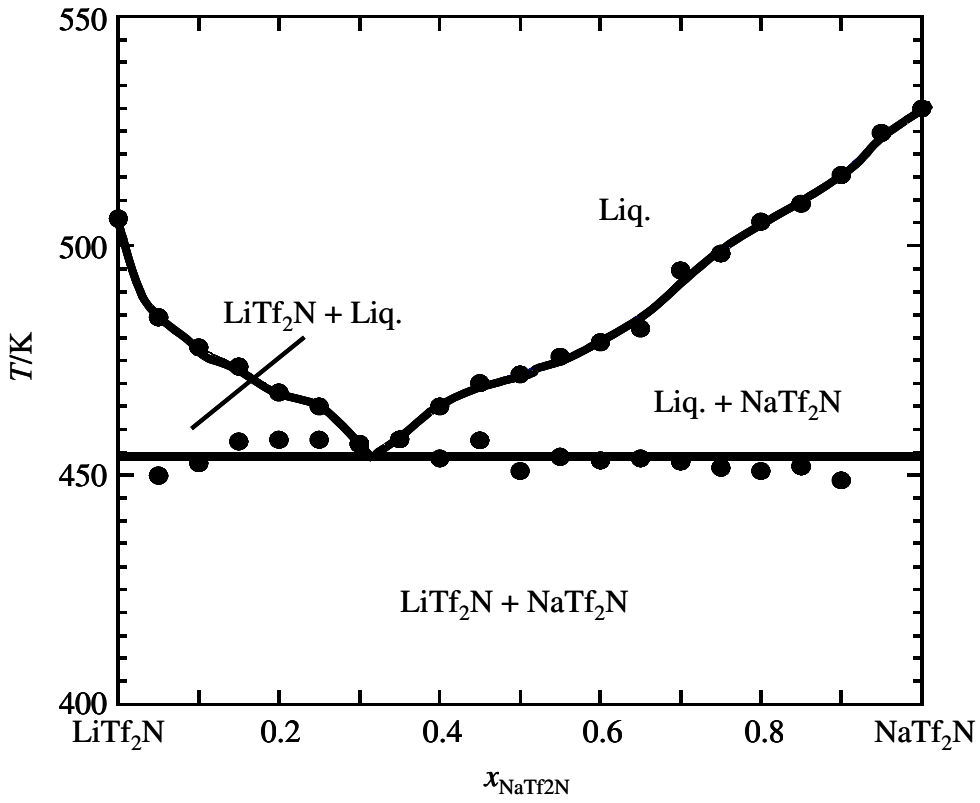

Figure 2. Phase diagram of $LiTf_2N$ + $NaTf_2N$

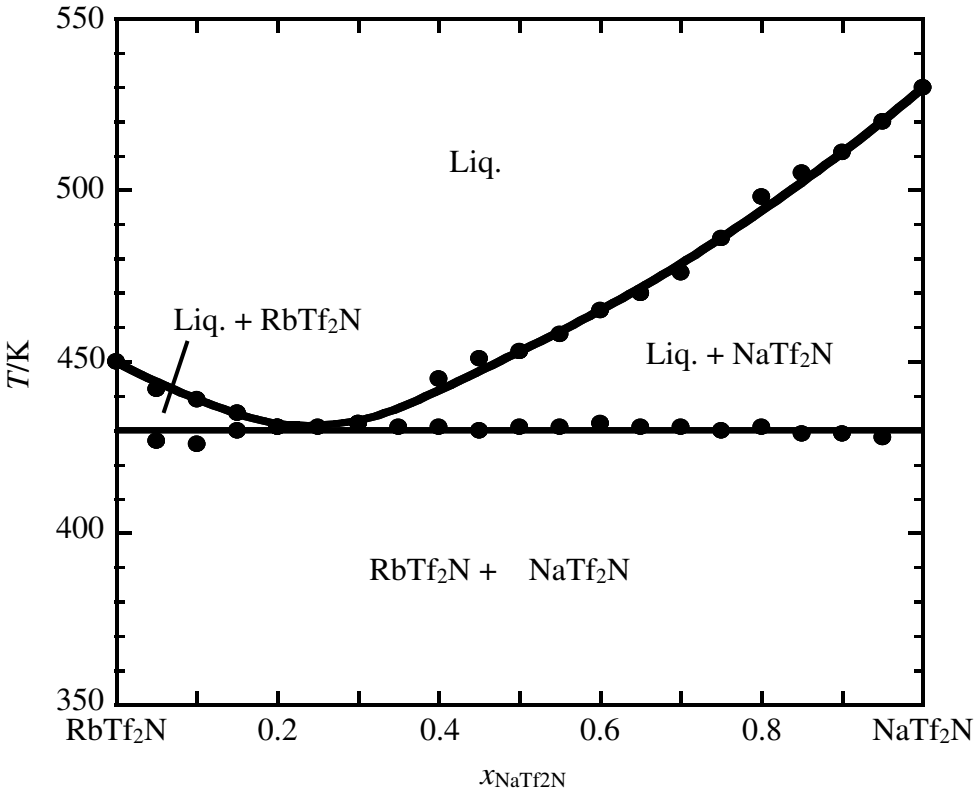

Figure 3. Phase diagram of $NaTf_2N$ + $RbTf_2N$.

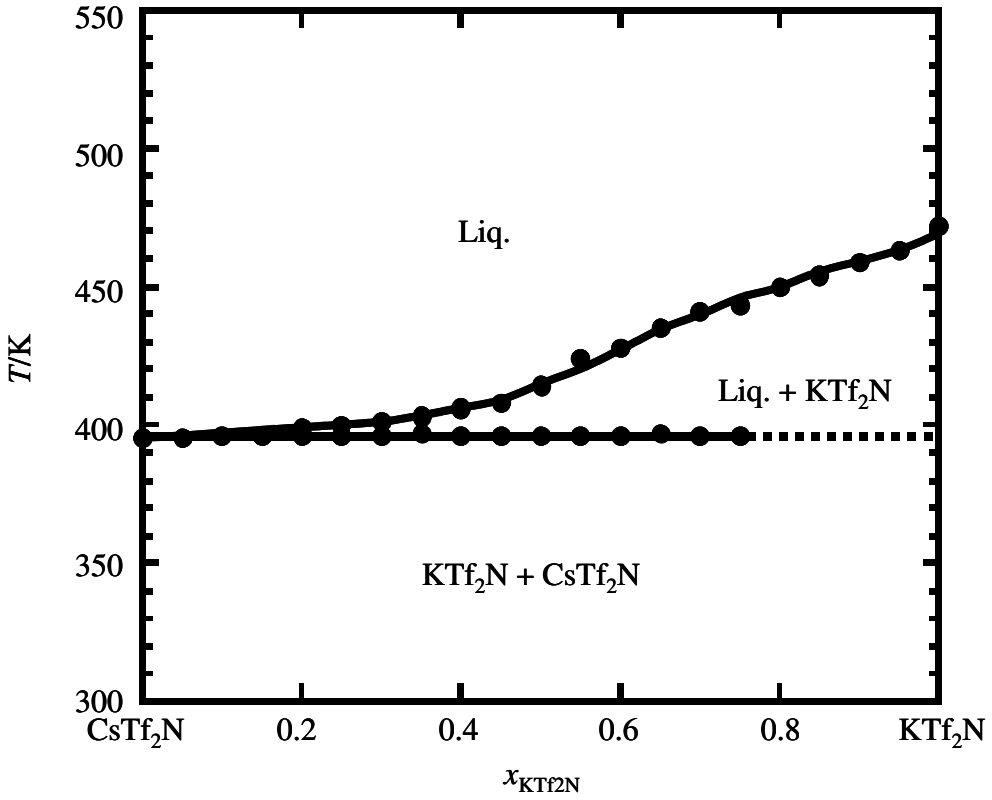

Figure 4. Phase diagram of KTf_2N + $CsTf_2N$.

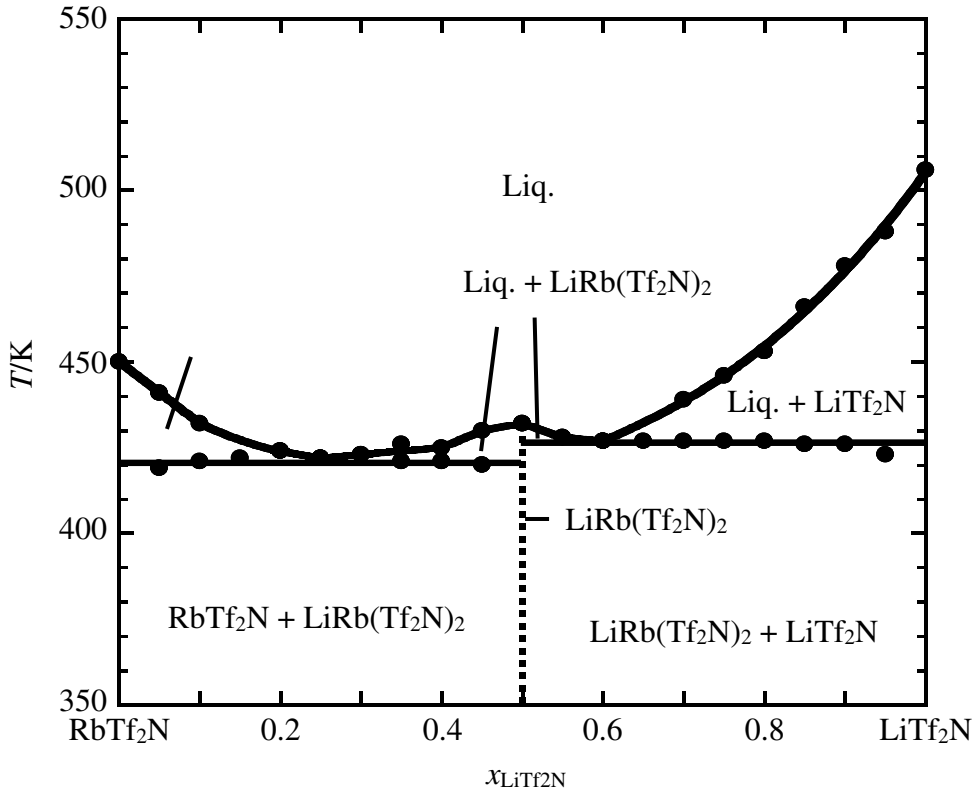

Figure 5. Phase diagram of $LiTf_2N$ + $RbTf_2N$.

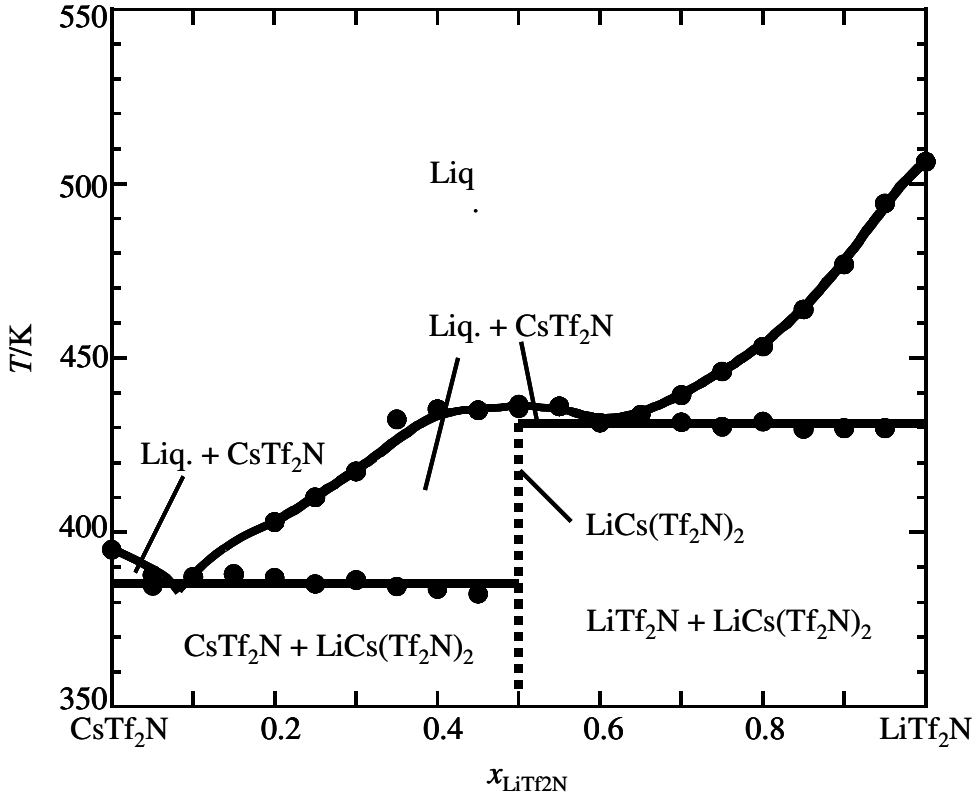

Figure 6. Phase diagram of $LiTf_2N$ + $CsTf_2N$.

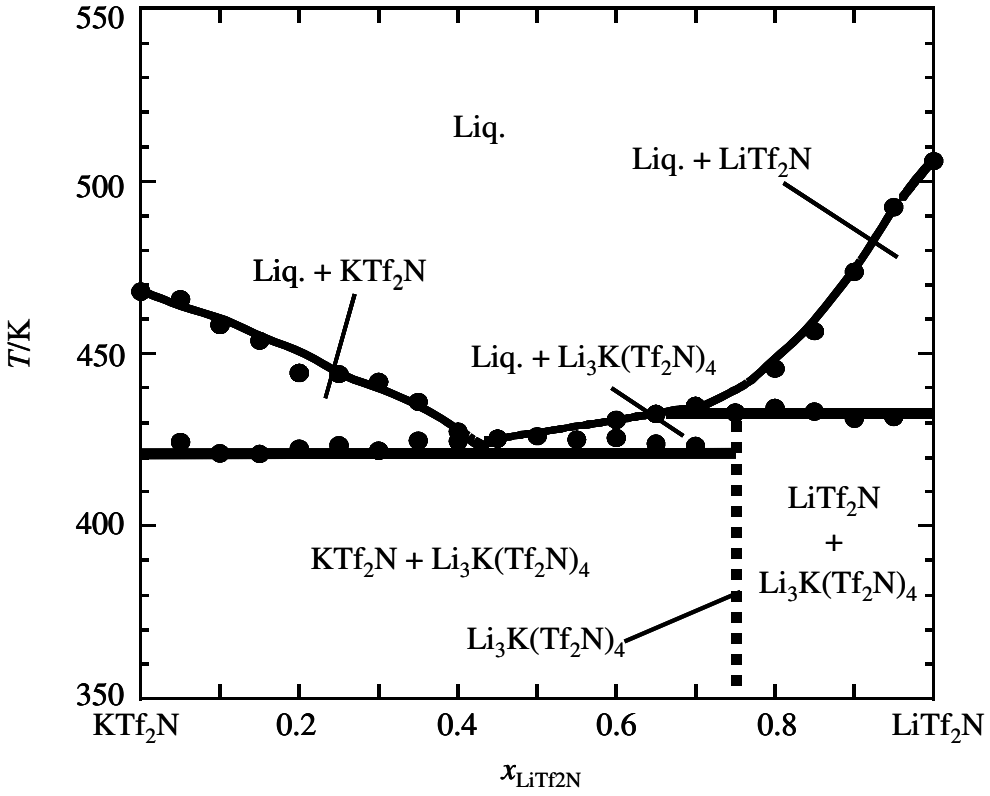

Figure 7. Phase diagram of $LiTf_2N$ + KTf_2N.

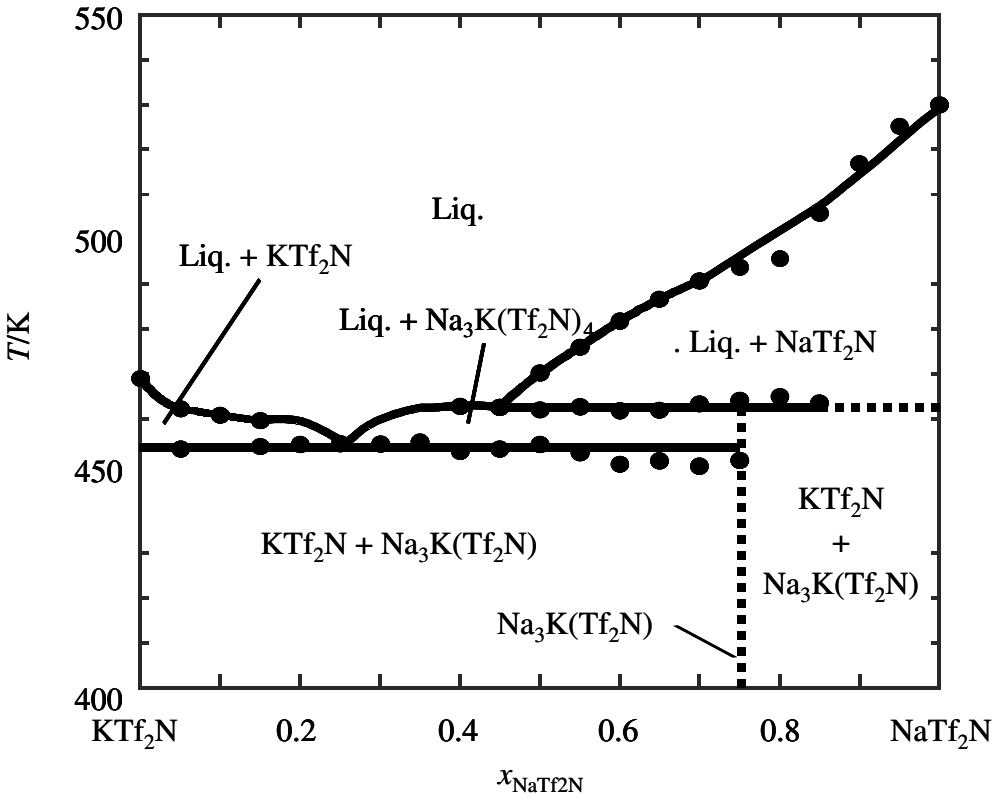

Figure 8. Phase diagram of $NaTf_2N$ + KTf_2N.

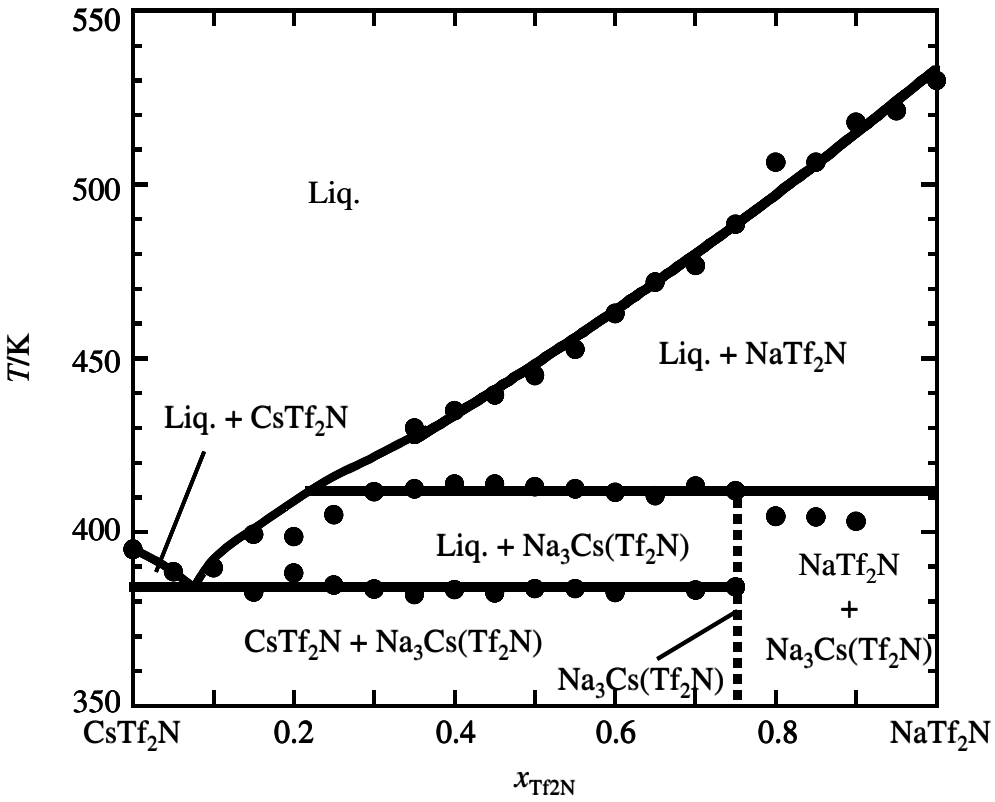

Figure 9. Phase diagram of $NaTf_2N$ + $CsTf_2N$.

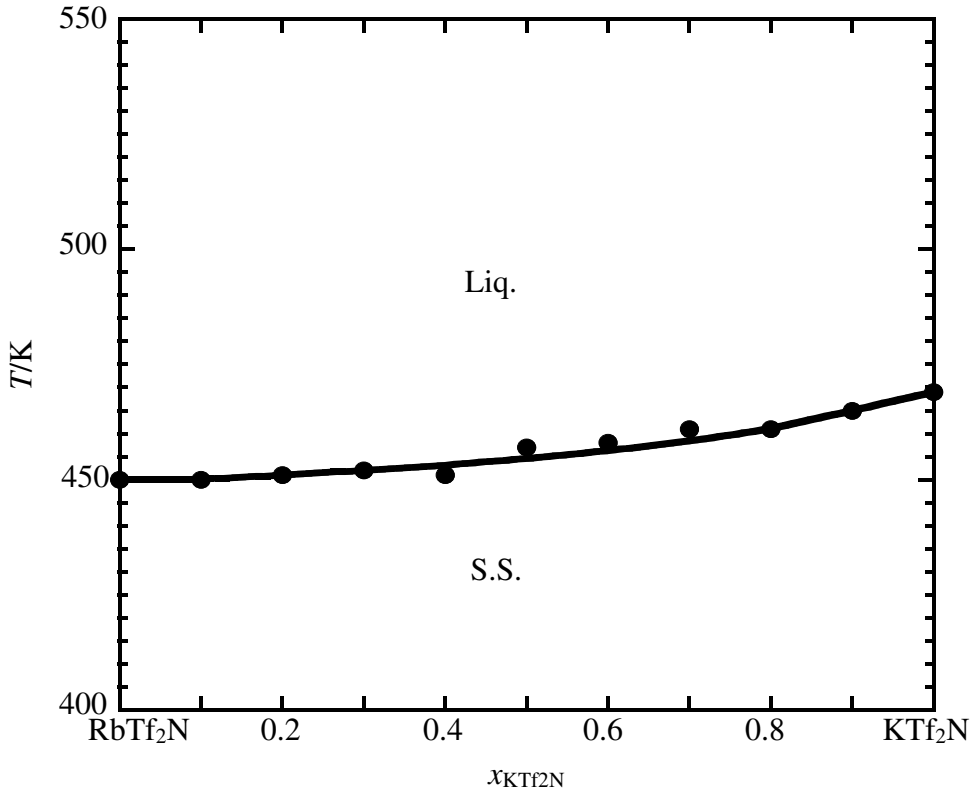

Figure 10. Phase diagram of KTf_2N + $RbTf_2N$.

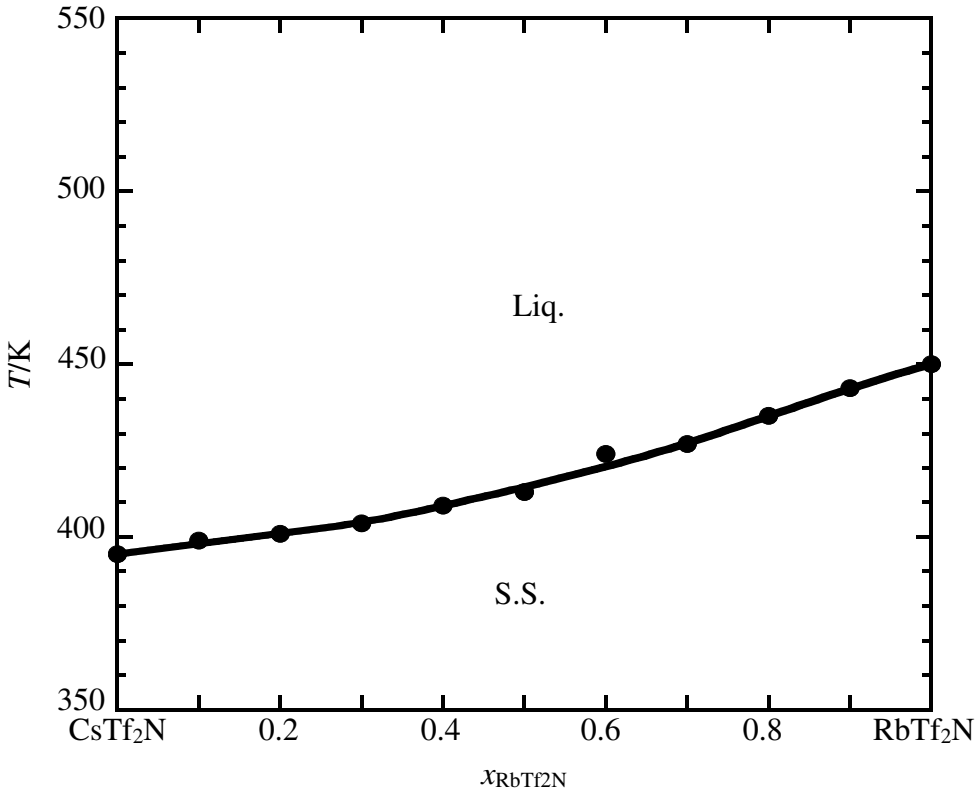

Figure 11. Phase diagram of $RbTf_2N$ + $CsTf_2N$.